Nonparabolic band effects in GaAs/Al$_x$Ga$_{1-x}$As quantum dots and ultrathin quantum wells

N. Schildermans, M. Hayne, and V. V. Moshchalkov

Pulsed Field Group, Laboratory of Solid State Physics and Magnetism, Katholieke Universiteit Leuven, Celestijnenlaan 200D,
B-3001 Leuven, Belgium

A. Rastelli and O. G. Schmidt

Max-Planck-Institut für Festkörperforschung, Heisenbergstr. 1, D-70569 Stuttgart, Germany
(Received 3 June 2005; revised manuscript received 20 July 2005; published 14 September 2005)

We have investigated the optical properties of unstrained GaAs/Al$_x$Ga$_{1-x}$As quantum dot/well systems with the aim of studying the influence of confinement on the effective exciton mass, as determined from the photoluminescence line shift in high magnetic fields ($\leqslant$50 T). The effective exciton mass is found to be more than twice the value for bulk GaAs. We attribute this to an enhanced nonparabolicity in the GaAs conduction band at the nanoscale.

I. INTRODUCTION

Nanosized semiconductor heterostructures are convenient systems to study confinement and quantization effects. At the same time these systems can be used to develop new opto-electronic devices.[1] Indeed, understanding of the quantum physics in these structures is necessary to control the performance of nanoscale devices and to design and fabricate new heterostructures with specific properties. Simple and frequently used theoretical models that describe the electron and hole properties in a semiconductor approximate the band structure by parabolic conduction and valence bands with constant electron and hole masses that depend on the curvature of the band. This parabolic band approximation, also called the effective mass approximation, works well in bulk materials and is also often used for the description of nanosized systems, with the electron and hole masses treated as constant input parameters equal to the bulk values. Deviations from the parabolic model are typically not considered in quantum well/dot (QW/QD) calculations based on effective mass approaches.[2–9] Here we show that nonparabolicity becomes crucially important in systems with dimensions $\leqslant$10 nm, and can increase the effective exciton mass by more than a factor of 2.

Confinement effects in QW/QD systems cause a shift of the energy levels, ΔE, depending on the effective mass of the confined particles. When the energy has a parabolic dependence on the wave vector **k**, then the energy states increase equally with confinement independent of **k**, without changing the dispersion in the conduction band. However, the conduction band is not parabolic in real systems, and the shift ΔE is **k** dependent, implying a substantial modification of the conduction band in low dimensional structures. Specifically, the Γ-conduction band, with a light mass, is more influenced by the confinement than the L and X bands. This results in a decreasing dispersion of the conduction band and a changing band curvature.[10] The deviation from the parabolic model, the nonparabolicity, increases when the structure size decreases and causes the effective electron mass to be dependent on the structure size.[10–13] The effects of confinement on the electron effective mass have already been studied theoretically for QWs[10–12] and quantum wires (QWRs);[13] these models indeed predict an increasing influence of nonparabolicity with decreasing dimensions. The increase in effective electron mass, due to nonparabolicity and wave function penetration, becomes significant in QWs thinner than 10 nm and this has been confirmed by several experimental studies.[14–16] An enhancement of the electron mass by 12% was measured with the Shubkinov-de Haas oscillation technique in a 5-nm-thick GaAs/Al$_x$Ga$_{1-x}$As QW.[14] An enhancement of up to 40% was observed using the same method in a 2-nm-thick GaAs/In$_x$Ga$_{1-x}$As/Al$_y$Ga$_{1-y}$As QW,[15] and a mass increase of 50% was measured, using cyclotron resonance, in a 1.5-nm-thick In$_{0.53}$Ga$_{0.47}$As/InP QW.[16]

Here we report magnetophotoluminescence (magneto-PL) results on unstrained GaAs/Al$_x$Ga$_{1-x}$As QD/QW systems. In most QD structures it is not possible to experimentally separate the effects of confinement on the band structure from material-related properties such as strain and intermixing. The principal advantage of the GaAs/Al$_x$Ga$_{1-x}$As structures studied here is that the two materials have almost identical lattice constants, such that they are unstrained and expected to have little or no intermixing. This makes them ideally suited for the study of pure confinement effects.[17] We have measured the effective exciton mass in such QDs and ultrathin QWs, and in both cases found values between 0.11 and 0.17 m_e (with m_e the free electron mass), more than twice the value for bulk GaAs of 0.056 m_e.[18] Thus, our results unequivocally demonstrate the important role band nonparabolicity effects must play in all semiconductor nanostructures with light (bulk) effective electron masses,[10] and particularly in quantum dots.

II. EXPERIMENTAL DETAILS

A. Sample preparation

The quantum structures were produced by using a modified self-assembling process, involving several steps in a single growth run. Samples are grown using solid-source molecular beam epitaxy, starting with the production of stan-
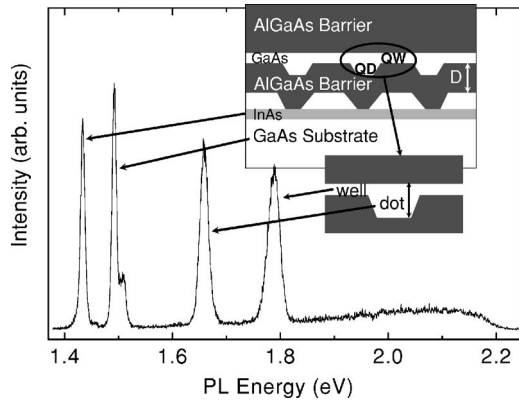
FIG. 1. Schematic drawing of the sample structure, together with a typical photoluminescence spectrum. The QDs, the ultrathin QW, and the lower barrier with varying thickness, D, are indicated. The QD thickness is also indicated and includes the QW thickness. The two peaks at higher energy come from the QW and QD structures, and are investigated here.

dard self-assembled InAs/GaAs (001) dots. *In situ* strain-enhanced etching preferentially removes the InAs dots and creates a surface with nanoholes. Depositing a thin $Al_{0.45}Ga_{0.55}As$ layer preserves the nanoholes, which are then filled with GaAs to make unstrained GaAs dots under a GaAs QW. The depth of the nanoholes depends inversely on the thickness D of the $Al_{0.45}Ga_{0.55}As$ layer. An $Al_{0.35}Ga_{0.65}As$ barrier and capping layers complete the structure.[17] A schematic drawing of the sample together with a representative photoluminescence (PL) spectrum is given in Fig 1. The PL spectrum consists of four sharp peaks that come from different parts of the sample. The first peak at the lowest energy side is the PL from the InAs wetting layer. The second one comes from the GaAs substrate. The two peaks at higher energies are from the GaAs quantum structures, with the QD peak at lower energy than the QW peak. The full width at half maximum of the QD PL is around 15 meV, which indicates that the size distribution of these dots is as good as most self-assembled QDs. The PL from both the QDs and the QW are measured in a single experimental run for each sample.

We investigated four QD/QW samples and one sample with only a QW, which was grown without the formation and subsequent etching of InAs QDs. The differences between the four QD/QW samples are the lower barrier, QW, and QD thicknesses, which are given in Table I. The sizes of the QDs are given by the shape of the $Al_{0.45}Ga_{0.55}As$ nanoholes,

TABLE I. Characteristics of the samples: QW, QD, and barrier thickness, D. The QD thickness includes the QW thickness, as indicated in the schematic drawing of Fig 1. The last sample is the reference QW, without QDs.

Sample number	1	2	3	4	5
D(nm)	5	7	10	15	7
QW thickness (nm)	1.75	1.80	1.85	1.86	2
QD thickness (nm)	6.56	5.96	5.13	4.50	-

which are determined by atomic force and scanning tunneling microscopy.[17] The total QD thickness is then the depth of the $Al_{0.45}Ga_{0.55}As$ nanohole plus the QW thickness, which is estimated by subtracting the nanohole volumes from the volume of the total amount of GaAs material deposited. Notice that the QD thickness depends inversely on the lower barrier thickness D.

B. Magnetophotoluminescence

The shift of the magnetophotoluminescence (magneto-PL) line in high magnetic fields was used to determine the effective exciton mass and the exciton radius in the QW and the QDs of these structures.[19] Magnetic fields (B) were generated in pulses of 20 ms with a pulsed field coil in combination with a 5 kV capacitor bank. Three measurements with a photon integration time of 0.5 ms were made during one pulse, with a field variation of maximum 5% during each 0.5 ms time interval. The experiments were carried out in a He^4-bath cryostat at 4.2 K, using an argon-ion laser at a wavelength of 514 nm (at power densities between 9 and 30 W/cm^2) to excite the electrons. The laser light was transmitted to the sample in the cryostat with a single 200-μm core fibre, while the emitted light from the sample was collected by six fibers for transmission to the spectrometer. The PL was analysed by a spectrometer and an intensified charged-coupled-device (CCD) detector.

The peak position, E_{CM}, of the PL spectrum is obtained by defining the center of mass of the measured PL spectrum, using the expression

$$E_{CM} = \frac{\int I(E)E dE}{\int I(E)dE}, \quad (1)$$

in which $I(E)$ is the PL intensity at the energy E. The PL energy versus field dependence is parabolic at low and linear at high fields. The parabolic-linear $E(B)$ crossover occurs at a field, B_c, which depends on the exciton radius and gives information about the confinement in the direction perpendicular to the applied field. Typical curves for the QDs and the QW are given in Fig. 2. The curves are fitted in a single procedure with the function[19]

$$E_{CM} = E_0 + \frac{e^2 \langle \rho^2 \rangle}{8\mu} B^2 \quad \text{for } B < B_c = \frac{2\hbar}{e\langle \rho^2 \rangle},$$

$$E_{CM} = E_0 - \frac{\hbar^2}{2\mu\langle \rho^2 \rangle} + \frac{\hbar e}{2\mu} B \quad \text{for } B > B_c = \frac{2\hbar}{e\langle \rho^2 \rangle}, \quad (2)$$

yielding three parameters: the zero field PL energy E_0, the average exciton extent $\langle \rho^2 \rangle^{1/2}$, and the effective exciton mass, μ. Here, e is the electron charge and $\hbar$ is the reduced Planck constant. The effect of the Zeeman splitting is not taken into account in the fitting procedure, since the effect is quite small, although not completely negligible, and would introduce unnecessary additional fitting parameters. An estimate of the Zeeman contribution can be made using the ex-
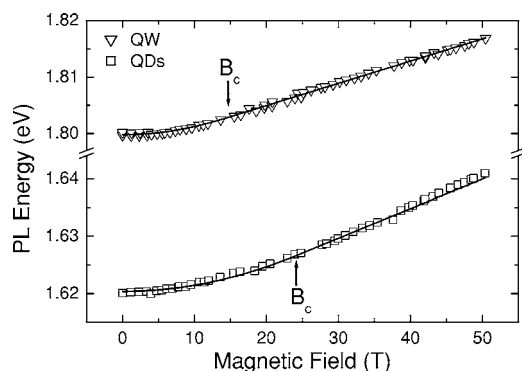
FIG. 2. Field dependence of the QW and the QD PL energies in sample 2 ($D=7$ nm) fitted with Eq. (2). The crossover field, B_c, is indicated in both cases. Note that the higher B_c for the QDs indicates the presence of confinement in the plane of the sample.

FIG. 3. Measured effective exciton masses, μ, of the QWs and QDs compared with theoretical models for the effective electron mass, m_e^*, in QWs[10] and in QWRs.[13] An estimated maximum value for the QD effective electron mass is also plotted.

citon g factors of -1.8 for a 2-nm QW and -0.8 for the 6.5-nm QD.[20,21] The maximum shift of the PL (i.e., at 50 T) due to low energy spin polarization is then found to be 2.5 and 1 meV for the QW and the QDs, respectively. Neglecting these shifts can cause an overestimation of the exciton mass of $<6\%$ in the case of the QDs, which is still in the error bars of the measurements. For the QWs the overestimation can be at most 15%. It should be noted that the polarization is small at low fields.

The smaller the quantum structures are, the higher the crossover fields, B_c, will be. Fields up to 50 T can be reached in the setup used, but the crossover field should be $\leqslant 35$ T to determine the mass reliably, corresponding to an exciton radius of $\geqslant 6.1$ nm. Using this method we can determine the in-plane effective exciton mass for the QWs and QDs, but not the out-of-plane effective mass, because the confinement in the growth direction is too strong.

The effective exciton mass, $\mu=\frac{m_e^* m_h^*}{m_e^* + m_h^*}$, with m_h^* the effective (heavy) hole mass, is measured in our experiments, whilst the effective electron mass m_e^* is calculated in the theory.[10–13] However, the effective exciton mass is always lower than m_e^* and the increase of μ is also smaller than the increase of m_e^*. Moreover, m_e^* is more likely to change than m_h^*, because the heavier hole is better confined and the hole wave-function extent is small; therefore, the hole is less influenced by confinement effects than the electron. Furthermore, since the valence band is not degenerate in quantum structures,[18] we assume that the exciton is a heavy-hole exciton, and we neglect the light holes. In general we can assert that the measured effective exciton mass is a *minimum* value for the effective electron mass. Thus, we can compare our results for the effective exciton mass with the theory for the effective electron mass, knowing that we can only *underestimate* the nonparabolicity effect.

III. RESULTS AND DISCUSSION

A. Ultrathin quantum wells

We start the discussion of our results with the measurements on the QWs, and will subsequently discuss the QDs.
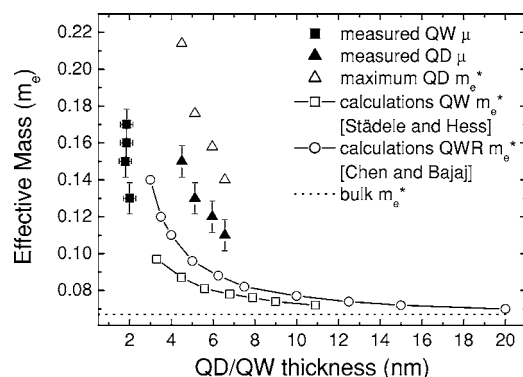
The measured in-plane effective exciton masses in the QWs are given in Fig. 3 (closed squares), together with the calculations of Städele and Hess[10] (open squares). We see a large increase of the effective exciton mass in the QWs with a width of 2 nm or less, as plotted in Fig. 3. Note that the QW thickness varies between 1.7 and 2 nm and the effective mass changes very fast, between 0.13 and 0.17 m_e, in this narrow range, which means that it is very sensitive to a small error in the QW thickness. As mentioned already in Sec. II B, the exciton mass can be overestimated due to spin polarization; however, since we measure the exciton mass, we find a lower limit for the electron mass.

As already mentioned, these samples are unstrained. Thus, only two effects could cause the mass enhancement, namely, nonparabolicity of the conduction band and wave-function penetration into the barriers. The importance of nonparabolicity increases when the well width decreases, as does the wave-function spillover into the barriers. Due to the limitations of the available magnetic field, we are not able to determine the extent of wave function in the growth direction. However, the absence of a parabolic-linear crossover before 35 T, indicates that the exciton radius can be at most 6.1 nm. Using this limiting value we have estimated the maximum wave-function spillover, approximating the wave function as a spheroid with a circular cross section in the plane of the QW and supposing that the penetration is equal in both barriers. We did not take the decaying amplitude of the wave function into account, but approximate it to be 1 within the spheroid and 0 elsewhere. This is certainly a crude estimate, but sufficient for our purposes. It is found that 40% of the wave function penetrates into the barriers at both sides, so the maximum penetration is 80%. The effective electron mass then becomes $m_e^* = P_W m_W^* + P_B m_{B_U}^* + P_B m_{B_L}^*$, with P_W and P_B the probabilities of the electron to be in the well or in the barriers.[18] The masses m_W^*, $m_{B_U}^*$, and $m_{B_L}^*$ are the effective electron masses for bulk materials in the QW, i.e., 0.067 m_e, and in the upper and lower barriers respectively. The effective electron mass in $Al_x Ga_{1-x} As$ depends on the Al-concentration x according to $m_{AlGaAs}^* = 0.067(1-x) + 0.154x$ and is thus 0.096 m_e for the upper barrier and 0.104 m_e for the lower barrier.[18,22] We thus find that the

maximum wave-function penetration of 80% corresponds to an effective electron mass increase of 40% and an effective exciton mass increase of about 30%, using 0.5 m_e for the heavy-hole mass and neglecting the light holes. This effect is certainly important in thin QWs, but it cannot explain the total mass increase of at least 120% that we observe. *We therefore conclude that nonparabolicity is the main cause of the mass enhancement*. Indeed, as shown in Fig. 3, our QW results follow the trend of the theoretical model, which is in good agreement with most experimental data to date.[14] Unfortunately, no theoretical predictions or experimental results are found in literature for QWs of only 2 nm or thinner, so no further quantitative comparison can be made. Existing models are not expected to be valid for ultrathin quantum structures because of the increasing influence of the wavefunction penetration, which is not taken into account.[13]

B. Quantum dots

We now discuss the effective exciton masses measured in the QDs, which are also shown in Fig. 3 (closed triangles). The exciton masses are in a range of 0.11 to 0.15 m_e, neglecting the effect of the Zeeman splitting. We will start the discussion with the influence of the wave-function spillover. The wave-function penetration is estimated in the same way as for the QWs. The QDs are shallow with an approximately triangular cross section in the [110] direction and an elongated lateral shape,[17] but for the estimation of the wavefunction spillover they are approximated as flat boxes with average lateral sizes of 16 nm width and 44 nm length. The wave-function penetration is smaller than for the wells since the dots are thicker, and comes to about 30–40%. The effective electron mass increase due to this effect is between 15 and 20 %, and thus relatively small in comparison with the observed enhancement of the effective exciton mass. It should be noted that the mass enhancement due to wavefunction penetration is almost the same for the different samples, while the total mass enhancement strongly depends on the QD size, consistent with nonparabolicity as the primary driving mechanism.

The effective exciton mass is the minimum value for the effective electron mass, but we can also estimate a maximum value, supposing that the effective hole mass in the quantum structure is the same as the bulk value, i.e., 0.5 m_e (for a heavy hole). The maximum effective electron masses for the QDs are found to be between 0.14 and 0.21 m_e (Fig. 3). The effective electron masses in the $Al_xGa_{1-x}As$ barriers are 0.096 or 0.104 m_e, depending on the Al-concentration x. This means that even the minimum effective electron mass values (the effective exciton mass values) are all bigger than the effective electron masses in the barriers, i.e., wave-function spillover can never cause a mass increase of more than 55%. This is convincing evidence that nonparabolicity, and not the wave-function spillover, is the main reason for the mass enhancement.

We now compare these results with effective electron mass calculations for $GaAs/Al_{0.3}Ga_{0.7}As$ QWRs[13] (open circles in Fig. 3), since there are, to our knowledge, no theories available for QDs. Chen *et al.* calculated the effective electron masses in QWRs with a square cross section and this theory predicts a larger mass enhancement than in QWs, due to the confinement in two directions. A stronger effect can thus be expected when there is confinement in three directions, exactly as observed here. Indeed, even in these flat dots, where the lateral dimensions are relatively large, the additional confinement has a clear effect on the effective exciton mass, the measured effective mass values being comparable to those of the thinner QWs. The difference between the effective exciton masses in the QDs and the calculated electron masses in the QWR is remarkably big in comparison to the QW-QWR effective electron mass increase. This difference is caused by the influence of the wave-function penetration, which is not taken into account in the calculations.

IV. CONCLUSION

In conclusion, we have studied the effects of conduction band nonparabolicity on the exciton properties in GaAs/AlGaAs QDs and very thin QWs and in QDs using high field magneto-PL. It is found that the influence of nonparabolicity becomes very important when the size of the quantum structure decreases in one direction, as observed in the QWs. The nonparabolicity effect is stronger when the dimensions of a structure decrease in all directions, as we observed for the QDs, doubling the exciton mass for QD thicknesses as large as 6 nm. These results demonstrate the increasing influence of the band nonparabolicity on the effective exciton mass in QDs, and indicates the necessity for theoretical calculations of this effect in QDs.

[1] D. Bimberg, M. Grundmann, and N. N. Ledentsov, *Quantum Dot Heterostructures* (John Wiley & Sons Ltd., New York, 1999).

[2] Lok C. Lew Yan Voon and Morten Willatzen, IEEE J. Quantum Electron. **35**, 1424 (2003).

[3] M. Tadic, F. M. Peeters, and K. L. Janssens, Phys. Rev. B **65**, 165333 (2002).

[4] M. Tadic, F. M. Peeters, B. Partoens, and K. L. Janssens, Physica E (Amsterdam) **13**, 237 (2002).

[5] R. Cingolani, R. Rinaldi, H. Lipsanen, M. Sopanen, R. Virkkala, K. Maijala, J. Tulkki, J. Ahopelto, K. Uchida, N. Miura, and Y. Arakawa, Phys. Rev. Lett. **83**, 4832 (1999).

[6] S. J. Cheng, W. Sheng, and P. Hawrylak, Phys. Rev. B **68**,

235330 (2003).

[7] A. Wojs, P. Hawrylak, S. Fafard, and L. Jacak, Phys. Rev. B **54**, 5604 (1996).

[8] D. Smirnov, S. Raymond, S. Studenikin, A. Babinski, J. Leotin, P. Frings, M. Potemski, and A. Sachrajda, Physica B **346&347**, 432 (2004).

[9] O. Stier, R. Heitz, A. Schliwa, and D. Bimberg, Phys. Status Solidi A **190**, 477 (2002).

[10] M. Städele and K. Hess, J. Appl. Phys. **88**, 6945 (2000).

[11] U. Ekenberg, Phys. Rev. B **40**, 7714 (1989).

[12] L. C. Andreani and A. Pasquarello, Phys. Rev. B **42**, 8928 (1990).

[13] R. Chen and K. K. Bajaj, Phys. Rev. B **50**, 1949 (1994).

[14] H. Çelik, M. Cankurtaran, A. Bayrakli, E. Tiras, and N. Balkan, Semicond. Sci. Technol. **12**, 389 (1997).

[15] G. Hendorfer, M. Seto, H. Ruckser, W. Jantsch, M. Helm, G. Brunthaler, W. Jost, H. Obloh, K. Köhler, and D. J. As, Phys. Rev. B **48**, 2328 (1993).

[16] C. Wetzel, R. Winkler, M. Drechsler, B. K. Meyer, U. Rössler, J. Scriba, J. P. Kotthaus, V. Härle, and F. Scholz, Phys. Rev. B **53**, 1038 (1996).

[17] A. Rastelli, S. Stufler, A. Schliwa, R. Songmuang, C. Manzano, G. Costantini, K. Kern, A. Zrenner, D. Bimberg, and O. G. Schmidt, Phys. Rev. Lett. **92**, 166104 (2004).

[18] J. H. Davies, *The Physics of Low-Dimensional Semiconductors* (Cambridge University Press, Cambridge, 1998).

[19] M. Hayne, J. Maes, S. Bersier, M. Henini, L. Müller-Kirsch, R. Heitz, D. Bimberg, and V. V. Moshchalkov, Physica B **346&347**, 421 (2004).

[20] M. J. Snelling, E. Blackwood, C. J. McDonagh, R. T. Harley, and C. T. B. Foxon, Phys. Rev. B **45**, R3922 (1992).

[21] J. G. Tischler, A. S. Bracker, D. Gammon, and D. Park, Phys. Rev. B **66**, 081310(R) (2002).

[22] A. Franceschetti and A. Zunger, Phys. Rev. B **52**, 14664 (1995).